

Physical Actions in Biological Adhesion

E. EVANS

*Departments of Pathology and Physics,
University of British Columbia,
Vancouver, B.C., Canada V6T 2B5*

Contents

1. Preface: Biological view of adhesion	725
2. Introduction: Physical view of adhesion	726
3. Mechanics of adhesion: Macroscopic view	728
4. Membranes: Macrocolloids	734
4.1. Van der Waals attraction	735
4.2. Electric double layer repulsion	736
4.3. Entropy-driven repulsion between flexible membranes	736
4.4. Depletion driven attraction	737
5. Biological adhesion: Contact formation	740
5.1. Spreading by cytoskeletal contraction	740
6. Biological adhesion: Focal bonding	742
6.1. Strength of attachment	742
6.2. Microscopic dynamics of rupture	745
7. Biological adhesion: Macroscopic contacts	746
7.1. Contour roughness, mechanical stiffness and impingement	746
7.2. Mesoscale mechanics of fracture	750
8. Summary comment	752
Acknowledgement	752
References	752

1. Preface: Biological view of adhesion

Tissue assembly (development) and other biological functions (like identification and removal of alien organisms in immune defense) involve complex adhesive interactions. Biologists have identified and isolated many molecular 'adhesins' responsible for cellular adhesion processes [1]. Classification of receptors and ligands in cell adhesion has become a major enterprise in mammalian biology. The list is long and some of the evidence is circumstantial (e.g., 'cell sticking versus nonsticking' in relation to competitive binding of ligands to putative sites of adhesive activity). Unfortunately, little is known about the microscopic bonding actions (physical-chemical) between cell adhesion molecules. In any case, the present view of cell adhesion in biology is *briefly* outlined here to provide a comparative perspective for the discussion of physical actions that will follow.

The collective dogma (for mammalian cells) is that cell adhesion molecules fall into four *groups*.¹

- (i) *Integrins*: a family of membrane glycoproteins composed of α and β subunits. The ligand binding site is formed by both subunits; the cytoplasmic domains are thought to be connected to the cell cytoskeleton. Integrins are receptors for extracellular matrix proteins. In many instances, a specific amino acid sequence (Arg-Gly-Asp = RGD) is believed to participate in recognition [2]. Subfamilies of integrins are distinguished by their β subunits: $\beta 1$ (CD29) – VLA proteins; $\beta 2$ (CD18) – leukocyte integrins; and $\beta 3$ (CD61) – cytoadhesins. The $\beta 1$ subfamily binds to extracellular matrix proteins fibronectin, collagen, and laminin. The $\beta 2$ subfamily is unique to leukocytes [3] and is thought to be important in converting circulating leukocytes to adherent tissue cells. The best characterized molecule of the $\beta 3$ subfamily is glycoprotein IIb/IIIa (α IIb $\beta 3$) (CD41/CD61), found exclusively on platelets and megakaryocytes. Glycoprotein IIb/IIIa plays a central role in platelet aggregation and clotting.
- (ii) *Selectins*: another family of calcium-dependent membrane glycoproteins. To date, selectins have been found only on circulating cells and endothelium. LAM-1 (LECAM-1), expressed on neutrophils, monocytes and most lymphocytes, facilitates binding to endothelium during lymphocyte recirculation and neutrophil emigration at inflammatory sites. ELAM-1 expressed on activated endothelial cells promotes the adhesion of leukocytes. 'Rolling' attachment of

¹ The author is grateful to his colleague and collaborator Dr. Susan Tha for providing the summary paraphrased in this paragraph.

leukocytes to endothelium seems to be mediated by selectins whereas ‘spreading’ adhesion appears to require $\beta 2$ integrins LFA-1 and Mac-1 via ICAM-1 [4].

- (iii) *Ig superfamily*: a diverse group of molecules whose structure resembles a sandwich of β -pleated sheets with disulfide bonds. The prototypical molecule is immunoglobulin. N-CAM is also a member of this superfamily [15]. Other Ig superfamily molecules function in immune response [6]. Lastly,
- (iv) *Cadherins*: a separate family of cell adhesion molecules without structural homology to other adhesion molecules [7]. Cells in solid tissues express at least some member of the cadherin family all of which exhibit calcium-dependent homophilic binding. Even though the size of the cytoplasmic domains vary greatly between these groups of cell adhesion molecules, all possess massive extracellular domains that extend prominently from the bilayer core of the membrane.

Other than for surface recognition, it is not clear why cells require a plethora of ‘sticky’ molecules (many types reside on the same cell) *or* what differences exist in physical strength of attachment amongst these ‘adhesins’? One characteristic is common to all specific adhesion sites on cells: i.e. the surface density is relatively low. On the average, tens of nanometers separate adhesion sites ($\sim 10^4$ lipids per site). As will be discussed, the paucity of potential attachments leads to complex mechanics of adhesion and often to catastrophic effects when adherent cells are separated.

2. Introduction: Physical view of adhesion

Exposure of the underlying physics in biological adhesion is difficult because of strong ‘coupling’ between cellular biochemistry, structure, and microscopic action. Idealized concepts only provide a phenomenological characterization of adhesion embodied in an ‘adhesion energy’ w_a (energy/unit area of contact). The view is predicated on the assumption that interfaces are smooth and adhere by intimate-uniform contact. Furthermore, the incremental energy w_a gained in contact formation is assumed to equal the mechanical energy w_f required to separate (‘fracture’) the contact: i.e. the process is energetically reversible ($w_a \equiv w_f$). Ideal adhesion of smooth contacts is the physical metaphor for ‘wetting-like’ adhesion originally developed in the 19th century [8] to describe spreading and contact angle behavior of liquid drops on solid substrates (or shapes of immiscible liquid interfaces). To some extent, the classical concept can be useful to model adhesion of liquid-like membranes that possess microscopically smooth surfaces. For instance, adhesion of lipid bilayer vesicles driven by colloidal-type attractions can be represented by a reversible adhesion energy related to microscopic physical forces between the surfaces. (*But* even for ‘smooth’ vesicle adhesion, the connection between macroscopic adhesion energy and microscopic interactions is obscured by hidden thermal excitations.) Situations of ‘ideal adhesion’ are easy to recognize since contacts spread spontaneously without mechanical impingement (‘push’) and the spreading actions

(‘wetting’) create membrane tensions. However, the nonspecific attractions that produce ideal adhesion between lipid bilayer vesicles do not drive cell adhesion in biology!

The fluid-like property of cell interfaces has stimulated several kinetic and thermodynamic models for cell adhesion [9]. These elegant developments have been extensively parameterized to represent a wide range of chemical features which leads to a rich spectrum of predictions. As with the classical adhesion energy approach, the models are based on a smooth surface abstraction for contact; and the kinetics are essentially near equilibrium processes. Consequently, the models must be regarded as primarily phenomenological. An important conclusion from thermodynamic models is that the spreading energy at full equilibrium is scaled by the effective surface pressure of adhesion sites: i.e. $w_a \sim \tilde{n}_B kT$ where \tilde{n}_B is the surface density (number/area) of adherent receptors [10]. The free energy of binding determines the fraction of bound adhesion sites at equilibrium; but the energy increment gained as bonds form balances the energy increment lost as bonds dissociate. Only entropy confinement is left to expand the contact. However, far from equilibrium, the mechanical work to separate the contact w_f approaches a limit characterized by the binding energy [10]. The caveat for biological cell adhesion is that receptor densities are usually very low ($< 10^{11}/\text{cm}^2$). Thus, the equilibrium energy scale for spreading is weak ($< 4 \times 10^{-3} \text{ erg}/\text{cm}^2$) in comparison to mechanical energies for deformation of the cell cortex.

Biological cells adhere to other cells or material substrates by completely *nonideal* processes. Attraction appears to be short range and localized to molecular-focal attachments (e.g., created by molecular bridges with agglutinins or direct bonds with intrinsic cell adhesion molecules). Interfacial forces of attraction between cells are not sufficient to pull the surfaces together. Clear evidence of this feature is that cells normally do not spread spontaneously on a substrate unless pushed into contact by external forces (mechanical impingement). Left alone, cells increase contact area either slowly through structural relaxation *or* rapidly by active motility. The behavior is simple: cells stick where they ‘crawl, flow, or are pushed’!

Most receptors and molecular adhesion sites on cell surfaces are relatively mobile; thus, it is expected that (given time) the focal character of intersurface bonding should be dispersed by lateral diffusion. Eventually, equilibrium should be reached where regions of contact are uniformly bonded. Based on measurements [11] of receptor diffusivity ($> 10^{-11} \text{ cm}^2/\text{sec}$) and characteristic lengths of 10^{-4} cm , only a few minutes should be required to reach this fully-bound state. In fact, receptor diffusion does appear to promote large regions of adherent contact for fluid-like interfaces with high densities of adhesive ligands (e.g., agglutination of lymphocytes by lectins – see Bongrand chapter and ref. [12]). On the other hand, unstimulated cells often take many hours to spread on surfaces even though the cells adhere immediately at a few points *or* can be made to adhere strongly by mechanical impingement of the cell against the substrate. Hence, biological cell adhesion seems to be ‘kinetically trapped’ to a great extent, much more than can be accounted for by diffusive limitations. Kinetic restrictions and strong focal bonding between cell membranes show-up in physical studies of cellular adhesion as irreversible behavior: i.e. little

(if any) detectable tendency (affinity) to spontaneously spread *but* strong force is needed to subsequently detach an adherent cell ($w_a \ll w_f$). Indeed, the strength of attachment after contact can be enormous – greater than the structural integrity of the cell material; and separation often leads to material rupture of the interface [13].

This phenomenological scenario indicates that physical actions in cell adhesion can be conceptually partitioned into mechanisms that lead to ‘ideal’ and ‘nonideal’ behavior. However, significant aspects of adhesion in biology are peculiar to cellular biochemistry and specific types of substrates. These particular features will be ignored here in order to focus on the general mechanisms involved in all biological adhesion processes. Macroscopic energy densities for contact formation *vis a vis* separation provide the physical diagnostics of adhesion; thus, a brief review of the macroscopic mechanics of adhesion will be given first accompanied by examples of adhesion experiments.

3. Mechanics of adhesion: Macroscopic view

Cell structure is heterogeneous and anatomically complex, but the interior is often a soft liquid-like environment. Thus, mechanical stresses become distributed almost uniformly as hydrostatic pressure. The major stress variation occurs within a layer near the cell surface, i.e. the cell cortex, which can be as thin as a lipid bilayer ($\sim 40 \text{ \AA}$) or as thick as an actin meshwork ($> 10^3 \text{ \AA}$). Even so, the cortex thickness is usually much smaller than the radii of curvature that characterize the macroscopic cell shape. Because of this, stresses can be integrated through the cortex to create macroscopic force cumulants or resultants called ‘tension’ (force/length) that balance external forces to first order *plus* ‘moments of stress’ that contribute higher order bending corrections [14]. These resultants embody the mechanical opposition to deformation when cells adhere to surfaces or are forced to separate from contact. In the mechanical sense, the cell cortex is reduced to a thin shell, labeled as a ‘membrane’ by mechanicians [14]. However, the mechanical membrane includes the lipid bilayer, extrafacial glycocalyx, and subsurface cytoskeleton scaffolding – i.e. *everything* (including microscopic ‘roughness’) from the liquid-like cytoplasm to the external aqueous medium. Even though this region can exceed $10^2 \times$ the thickness of the lipid bilayer, it still behaves mechanically like a ‘membrane’ provided that the principal radii of curvature (R_1, R_2) for the cell shape exceed the thickness by an order of magnitude or more. Certainly, the mechanical membrane abstraction oversimplifies the stress distribution in some cells; but the approach provides an easily understood way to connect the macroscopic mechanics of cell deformation to microscopic physics of adhesion.

At mechanical equilibrium (where a cell is stationary or moving very slowly), adhesion is characterized macroscopically by the differential balance between mechanical work expended to deform the cell capsule *vis a vis* energy gained with interfacial contact. In situations of *strong* adhesion (where high tensions are involved), mechanical equilibrium of an adherent capsule is deceptively simple: i.e. the energy either gained (w_a) per unit area of contact formation or expended (w_f)

Fig. 1. *Strong* adhesion (adhesion energies $w_a > 10^{-3}$ erg/cm²) and spreading of a neutral lipid bilayer vesicle onto a stiff pressurized vesicle (diameters ~ 20 μm). The adhesion process is 'ideal' as verified by the reversibility of bilayer tension versus apparent contact angle θ_c ; tension is controlled by pipet suction pressure.

to separate a unit area of contact is directly proportional to the tension τ_m in the cortical shell or membrane,

$$\left. \begin{array}{l} w_a \\ w_f \end{array} \right\} = \tau_m(1 - \cos \theta_c) \quad (1)$$

where $(1 - \cos \theta_c)$ is a mechanical leverage factor that depends on the 'apparent' contact angle θ_c between the capsule contour and substrate outside the perimeter of the contact as shown in fig. 1. As indicated, the proportionality also holds for both formation and separation (fracture) of contact; but the 'peeling' tension may not be the same as the 'spreading' tension. Also, it is important to note that the actual contact angle at the substrate is very small since the capsule contour is nearly tangent

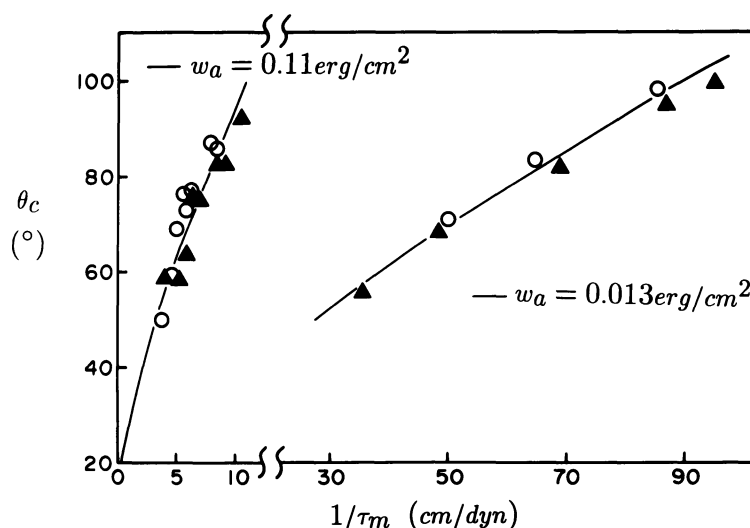


Fig. 2. Results for contact angles and bilayer tensions derived from adhesion experiments (cf. fig. 1) with neutral phospholipid vesicles in a 0.1 M NaCl solution. Attraction was driven by Van der Waals forces with stronger adhesion between phosphatidylethanolamine bilayers (data on the left) than between phosphatidylcholine bilayers (data on the right). Closed and open data symbols represent discrete equilibrium steps in the process of contact formation and separation, respectively. The solid curves are correlations predicted for uniform-fixed values of free energy reduction per unit area of contact (i.e. adhesion energy w_a).

to the surface within the contact region. The important features of adhesion for membrane capsules are illustrated by the example in fig. 1 of lipid bilayer vesicles drawn together by Van der Waals attraction. In fig. 1, the angle appears distinct because cortical bending stiffness is overwhelmed by the tension force. Clearly, if 'bigger magnification' were possible, we would see a continuous bend of the contour to microscopic-tangential contact. The mechanical balance (eq. (1)) for *strong* adhesion of fluid-like capsules (shown in fig. 1) is demonstrated in fig. 2. These data were derived from measurements [15] of tension and contact geometry for adhesion of lipid bilayer vesicles driven by colloidal attraction.² Unlike *free* liquid interfaces, both bilayer tension and angle θ_c are variable; but the adhesion energy is uniform, constant, and reversible. The reason that the tension can vary is because the lipid bilayer is a tightly condensed material [16]. The tension is a stiff-elastic response to pressurization that arises when the vesicle area is required to increase as the adhesive contact spreads. Hence, the vesicle area: volume ratio is the principal determinant of the contact geometry (i.e. angle θ_c).

² The method for control of the adhesion process involved manipulation of vesicles by micropipets. The vesicles were maneuvered into close proximity, allowed to adhere, and pressurized by pipet suction. The tension in each vesicle was regulated by suction pressure. One vesicle was stiffened by high tension whereas the other vesicle was allowed to spread on the stiff vesicle to an extent limited by a low bilayer tension (fig. 1a). Reversibility of adhesion was verified by measurements of tension versus contact angle for both formation and separation of the contact. When released from the pipet, the adherent vesicle spread to maximum contact limited by fixed surface area and volume as shown in fig. 1b.

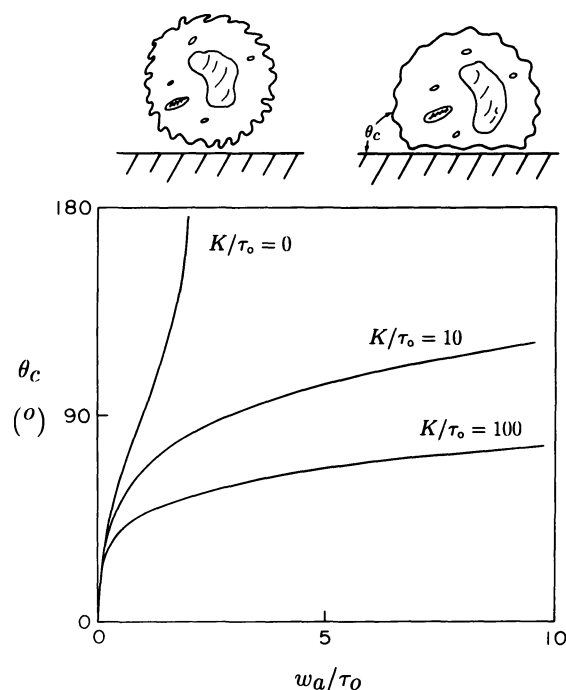


Fig. 3. Predictions of contact angle θ_c in relation to adhesion energy w_a for adhesion of a macroscopically spherical cell to a flat substrate. The cortex of the cell is assumed to possess an initial cortical tension τ_0 with an elastic expansion modulus K so that the tension in the cortex is given by $\tau_m = \tau_0 + K(\Delta\bar{A}/\bar{A})$. For biological cells, the increase $\Delta\bar{A}$ in macroscopic area is provided by smoothing of bilayer wrinkles as illustrated in the sketches.

For microscopically 'rough' cells, the effective area of the cell cortex can be increased by smoothing roughness which enables formation of large macroscopic contacts at low stress. The expansion of the cell cortex usually requires tensions that increase slightly with area, i.e. $\tau_m = \tau_0 + K(\Delta\bar{A}/\bar{A})$ where \bar{A} represents the macroscopic-scale (apparent) area of the cortex. The elastic constant K for lipid bilayers is very large (10^2 – 10^3 dyn/cm) and the 'natural' (reference) tension τ_0 is zero. Thus, the area of lipid bilayer vesicles remains essentially constant throughout the adhesion process. By comparison, the elastic constant for expansion of the cell cortex is usually much smaller ($< 10^{-2}$ – 10^{-2} dyn/cm for cells like blood phagocytes). Thus, by unwrinkling the superficial bilayer, the cortex area can easily be enlarged to allow adhesive contact. In living cells, these properties appear to be regulated by contractile processes in the cortex. The relationship between adhesion energy, cortical tension, and apparent contact angle θ_c is modeled in fig. 3 for adhesion of a macroscopically spherical cell to a flat substrate. This relation shows why smooth lipid bilayer spheres ($K \gg w_a$) only adhere with small contact areas ($\theta_c < 30^\circ$).

For simple membrane capsules with excess surface area, a subtle feature of *strong* adhesion is that the membrane may 'self adhere' as well as spread on another sub-

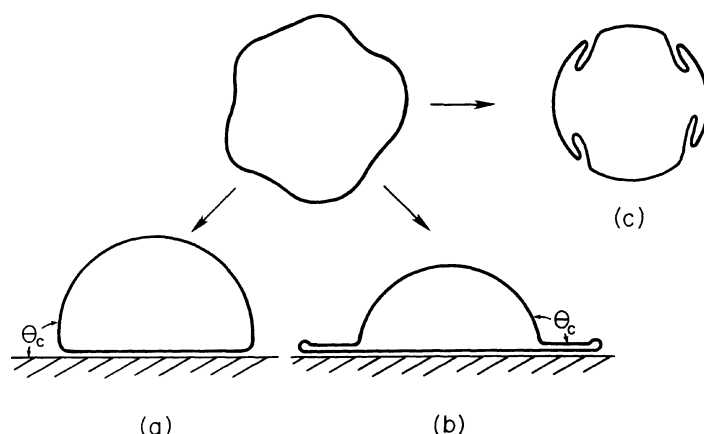


Fig. 4. Illustration of the competition between substrate adhesion and 'self' adhesion for a flexible membrane capsule with excess surface area. (a) Equilibrium shape of the capsule in the regime dominated by substrate attraction. (b) Equilibrium shape when membrane 'self' adhesion energy w_m is comparable to substrate adhesion energy w_a . (c) Equilibrium shape driven by 'self' adhesion without contact to the substrate.

strate. This situation is shown schematically in fig. 4. For strong adhesion (where bending rigidity is negligible), there is a critical angle θ_c^* beyond which the membrane can 'lap onto itself' driven by a self attraction energy w_m . Simple energetics for fluid membranes predict that the transition illustrated in fig. 4a→b should occur when,

$$\cos \theta_c \leq (w_m/w_a - 1)/(w_m/w_a + 1) \quad (2)$$

governed by the ratio w_m/w_a of self attraction to substrate attraction energies. An obvious corollary to the situation depicted in fig. 4b is self adhesion without contact to a substrate (fig. 4c). Clearly, this type of behavior is possible when the membrane tension (determined by pressurization of the capsule) falls to the level of the self attraction energy (i.e. $\tau_m \simeq w_m$). There are many geometric variations on this self adhesion theme. Because biological membranes are optically invisible, self adhesion is most easily recognized when a capsule appears to stop spreading on a substrate even though additional contact area is made available by reduction in volume. Self adhesion behavior is frequently observed in experiments with lipid bilayer vesicles. For example, it is difficult to achieve adhesion between weakly attracting vesicles of different compositions when self attraction of each membrane is stronger. Self adhesion requires that elastic energies of deformation be small compared with the attraction energies. As such, fluid membrane interfaces with weak bending rigidities are most susceptible to self adhesion – especially when membrane attractions are *strong*.

As membrane attraction weakens, bending rigidity as well as other 'stiffnesses' in the capsule shell lead to significant deviation from the classical energetics for a 'fluid interface' represented by the Young–Dupre relation (eq. (1)). When adhesion

Fig. 5. *Weak* adhesion (adhesion energies $w_a \ll 10^{-3}$ erg/cm²) of a lipid bilayer vesicle to a stiff pressurized vesicle (diameters ~ 20 μ m) in 0.1 M NaCl. (Here, the neutral lipid bilayers were doped with a small percentage ($\sim 5\%$) of negatively charged lipid to reduce attraction.) The continuous bend of membrane to the contact zone demonstrates the bilayer bending rigidity and exposes the parallel contact between the membrane surfaces.

is *weak*, the small region of membrane bending can reach macroscopic dimensions. The weak regime of adhesion is demonstrated in fig. 5. Here, bending rigidity (higher order ‘moments’ of stress in the membrane or cell cortex) becomes comparable to the mechanical action of the tension force. Precise mechanical analysis of this situation is not trivial; major numerical computations are required to calculate the capsule geometry and energetic balance [17, 18]. However, a good first-order approximation [15] to the analysis is given by,

$$w_a - (w_a \cdot e_0)^{1/2} \simeq \tau_m(1 - \cos \bar{\theta}_c) \quad (3)$$

where $\bar{\theta}_c$ is the effective contact angle indicated by the flattened capsule shape (cf. fig. 5). The constant e_0 is the elastic bending energy threshold that must be overcome to initiate contact, i.e. $e_0 = k_c/2R^2$ with R as the characteristic capsule radius, k_c is the elastic modulus for bending. For smooth cell-size capsules, the threshold is extremely small when the rigidity is dominated only by the lipid bilayer $k_c \sim 10^{-12}$ erg [16] and $R > 10^{-4}$ cm ($e_0 \ll 10^{-4}$ erg/cm²); but the effect of bending stiffness remains important even when $w_a/e_0 \sim 10$ (as indicated by the ‘geometric mean’ of adhesion energy and bending energy threshold). (Note: the size of the bending-dominated contour follows from the mechanical boundary condition at the perimeter of the contact where tension, bending stiffness, adhesion, and membrane curvature are related by $1/R_c = \sqrt{2w_a/k_c}$, refs [17–18].)

The macroscopic relations for mechanical equilibrium, eqs (1) and (3), demonstrate that discrimination between ideal and nonideal adhesion behavior lies in observation

of both the tension induced by contact spreading *and* the tension required to peel the contact apart. Thus, if a cell is not stressed by natural contact spreading, the adhesion energy must be negligible. On the other hand, if large stresses are produced in the cell under mechanical detachment, the fracture energy is large. Turning now to the microscopic features of physical actions in adhesion, we begin with ideal processes driven by classical ‘colloid forces’. These forces act ubiquitously on particles suspended in liquid media. As we will see, colloid forces only govern adhesion for the simplest membrane structures (e.g., smooth lipid bilayers) *or* in unusual situations where large attractions persist at long range from the surfaces.

4. Membranes: Macrocolloids

Membranes are supermolecular assemblies of organic molecules localized to a thin interfacial layer – from 30 Å to > 500 Å in thickness. Thus, membranes are macrocolloids that act on each other *nonspecifically* through the classical interactions well-established from the study of particle suspensions (e.g., ink, milk, clays, etc.). The prominent attribute of colloid interactions is that they essentially superpose (neglecting subtle effects). The net interaction can be expressed by a force σ_n per unit surface area that depends only on separation ‘ z ’ between surfaces. Thus, adhesion is driven by a physical potential that cumulates the action of all the forces from macroscopic separations to microscopic contact. The reversible potential (adhesion energy w_a) represents the energetic balance between attractive and repulsive interactions, i.e.

$$w_a = - \int_{\infty}^{z_c} \sigma_n dz. \quad (4)$$

Colloid interactions are commonly classified according to their range of action: *Long range* forces include electrostatic forces that decay exponentially ($\sigma_{es} \sim -P_{es} \times e^{-z/\lambda_{es}}$) in electrolyte solutions (e.g., the decay length $\lambda_{es} \sim 10$ Å and 0.1 M NaCl) and an inverse power-law (Van der Waals) attraction ($\sigma_{vdw} \sim A_H/z^2$) that extends effectively to macroscopic distances [19–21]. Van der Waals forces emanate mainly from the hydrocarbon core of the lipid bilayer [20]. In addition, steric exclusion of macromolecules from interfacial regions leads to long range ‘depletion’ attraction ($\sigma_M \sim \Pi_M e^{-z/\xi}$) that also decays exponentially with distance [22]. The decay length ξ is established by the correlation length for the macromolecular concentration field (typically the ‘size’ of the molecule, e.g., ~ 10 – 100 Å). Of the long range forces, Van der Waals attraction should dominate at large separations to draw membranes into adherent contact. For ‘atomically-smooth’ surfaces, the attraction creates large adhesion energies characteristic of liquid interfacial energies, e.g., ~ 50 ergs/cm² or more. However, as shown by the results in fig. 2, adhesion of ‘smooth’, neutral bilayers yields adhesion energies [23] that are orders of magnitude smaller (~ 0.01 – 0.1 erg/cm²).

Weak adhesion of neutral bilayers exposes the existence of a strong *short range* repulsion that prevents direct atomic contact. The short range force is often referred to as a ‘hydration’ force because it opposes condensation of all ‘hydrated’ molecular

interfaces, e.g., DNA, proteins, and surfactant lipid molecules (ref. [24]; see Rand and Parsegian chapter for elaboration). At small separations, repulsion between lipid bilayers becomes enormous! Several hundred atmospheres of pressure are required to push bilayer surfaces to $< 10 \text{ \AA}$; but the repulsion decays rapidly with exponential-like character ($\sigma_h \sim -P_h e^{-x/\lambda_h}$; decay length $\lambda_h \sim 2\text{--}3 \text{ \AA}$). The major consequence of the 'hydration' force is to stabilize neutral bilayer adhesion at separations between $10\text{--}30 \text{ \AA}$. Since Van der Waals forces decrease as $\sim 1/\text{distance}^2$, increasing separation from 'atomic' (1 \AA) distances to $10\text{--}30 \text{ \AA}$ diminishes the potential for adhesion by $1/100\text{--}1/1000$! Clearly, the 'hydration' force is essential for biological existence! Without it, bilayers (DNA and many proteins in solution as well) would collapse to condensed (dehydrated) states – destroying membrane structure and prohibiting biological function. Surprisingly, the physical origin of this force remains obscure at present. Several actions probably contribute to repulsion at short range: steric forces, solvent structure forces, electrostatic forces, etc., all of which are supported to some degree by experimental evidence. General study of colloid forces at *short* and *long* range is a major scientific activity which need not be reviewed here. The important question is: what roles do these ever-present actions play in biological adhesion processes?

4.1. Van der Waals attraction

The impact of colloid attraction depends strongly on the structure of the interface, principally topographical 'roughness' and electrical charge distribution. For example, smooth bilayer vesicles composed of electrically-neutral species (e.g., phosphatidylcholine PC and phosphatidylethalamine PE) adhere spontaneously in salt buffer ($> 10^{-3} \text{ M NaCl}$) as shown in fig. 1. However, the values of adhesion energy differ by an order of magnitude for the two lipids (PC $\sim 0.01 \text{ erg/cm}^2$ and PE $\sim 0.1 \text{ erg/cm}^2$). The reason is that the 'hydration' force is larger in PC bilayers; the bilayer separation is increased from $\sim 12 \text{ \AA}$ for PE to $\sim 27 \text{ \AA}$ for PC (as measured by X-ray diffraction methods – see Rand and Parsegian chapter). In contrast to lipid bilayers, biological membranes (even macroscopically smooth red blood cells) show *no* tendency to spontaneously spread on one another in 0.1 M NaCl ! The diminished attraction is not surprising since large extrafacial peptidoglycan moieties limit bilayer separations to $> 100 \text{ \AA}$. Hence, the adhesion potential due to Van der Waals forces should be extremely small (below 10^{-3} erg/cm^2 since the attraction diminishes as $1/\text{distance}^4$ at large separations). Therefore, macromolecular and other steric 'roughness' essentially quench Van der Waals forces so that they can usually be neglected in biological adhesion. However, this colloid action persists as a background attraction.

4.2. Electric double layer repulsion

Even though Van der Waals attraction can be neglected, electrostatic forces (mainly repulsive between cell surfaces because of the preponderance of negative charge) can play an important regulatory role in biological cell adhesion. Electrostatic repulsion in electrolyte solutions originates from osmotic pressure between surfaces created by

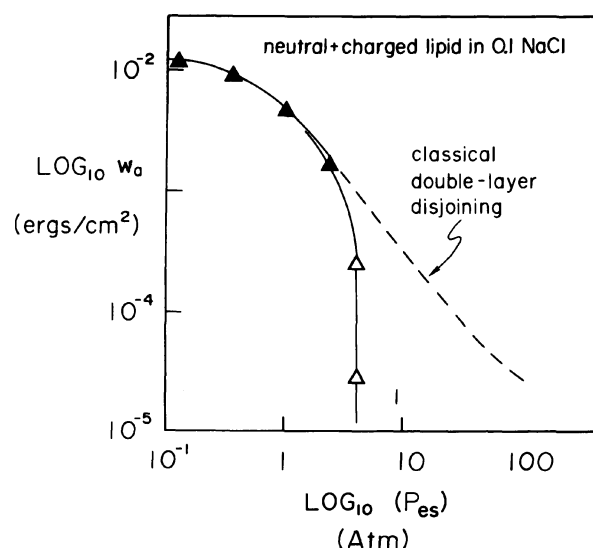


Fig. 6. Free energy potentials (adhesion energies) for adhesion of neutral lipid vesicles with small admixtures (0–6%) of electrically charged lipids in 0.1 M NaCl plotted as a function of the prefactor P_{es} for electric double layer repulsion. Solid triangles represent the strong adhesion regime where behavior is consistent with classical double layer predictions (dotted curve). Open triangles demonstrate the precipitous departure from classical disjoining that results from confinement of thermally excited fluctuations in membrane conformation. No attraction is observed between lipid bilayers that contain more than 1 charged lipid per 15–20 neutral lipids.

an excess of counterions drawn into the gap to neutralize the electric field created by surface charges. In 0.1 M monovalent salt solutions, the repulsion decreases rapidly with separation; the exponential decay length λ_{es} is about 10 Å. Because of the limited range, the principal effect of surface electrical charge is to reduce the adhesion potential near contact. This consequence is clearly shown by adhesion of lipid bilayer vesicles that contain small admixtures of negatively charged lipids (e.g., phosphatidylserine PS). Although weakened, the adhesion process remains 'ideal' – consistent with the direct dependence of electrostatic interaction on distance. Adhesion energies diminish rapidly with small increases in bilayer charge content [28] as shown in fig. 6 (e.g., a ratio of PC:PS of only 20 : 1 reduces the potential for adhesion by an order of magnitude from 10^{-2} to 10^{-3} erg/cm²). Biological cell surfaces possess much higher charge densities; but the charges are distributed over a thick glycocalyx outside the bilayer core. Because of 'screening' by ions in the electrolyte environment, repulsion acts primarily at short distances within about a decay length λ_{es} from the outer end of the glycocalyx and only charges that lie within a decay length from the end of the glycocalyx will contribute to the repulsion. Given a volumetric charge density $\bar{\rho}$ (i.e. charge/volume) in the glycocalyx, repulsion can be approximated by an interaction between surface charge densities of $\bar{\rho}\lambda_{es}$ 'pinned' to the periphery of each glycocalyx. (The magnitude of the prefactor P_{es} for repulsion ranges between 1–10 Atm (10^6 – 10^7 dyn/cm²) for surface charge densities in the range of 10^{12} – 10^{13} /cm² characteristic of cell interfaces.)

4.3. Entropy-driven repulsion between flexible membranes

A subtle feature of highly flexible membrane structures (e.g., lipid bilayers and red blood cell membranes) is that repulsion is greatly extended by confinement of thermal fluctuations [25–27]. Random microscopic variations in surface contour establish a significant configurational entropy for the membrane. The thermal-bending excitations are collective modes with a continuous spectrum of wavelengths from microscopic to macroscopic dimensions visible to an observer. For instance, red blood cell ‘flicker’ is the long wavelength manifestation of this ‘Brownian’ behavior. When membranes are forced into close proximity by attractive fields or mechanical impingement, entropy is confined (i.e. ‘heat’ is forced out) which requires mechanical work. For unstructured and noninteracting surfaces, the entropy reduction leads to a simple inverse-square law of steric repulsion (predicted many years ago by Helfrich – ref. [25]). However, of even greater consequence for *interacting* surfaces, the superposed action of *all* fields is altered to extend repulsion and diminish attraction [28–29]. The nonclassical effect is clearly evident in the precipitous quench of attraction between weakly charged vesicles (cf. fig. 6). In general, nontrivial calculations are required to predict steric effects when fields are presented; but qualitatively, there is a threshold-like behavior for flexible membrane capsules where the potential for adhesion is cut-off at a low level (e.g. $\sim 10^{-4}$ erg/cm²). Thermal fluctuations moderate adhesion of synthetic surfactant membranes and even highly flexible surfaces of mammalian red blood cells. However, in most cases, the effect can be neglected in the adhesion of cellular organisms. The cell cortex and cytostructure are too rigid to be displaced significantly by thermal excitations.

4.4. Depletion driven attraction

One type of colloid attraction can be significant in biological adhesion: i.e. macromolecular ‘depletion’ forces. The attraction is similar in origin and functional form – but opposite in sign – to electric double layer repulsion. Depletion forces are driven by *reductions* in osmotic pressure at the midpoint between surfaces which accompany steric exclusion of macromolecular solutes from nonadsorbant interfaces [22]. Because of random molecular motion, the exclusion fields interact at long range to attenuate the concentration in the gap even when separations exceed molecular dimensions. The correlation length ξ of the concentration field establishes the decay length for the depletion force and the osmotic pressure Π_M contributed by the macromolecular constituents sets the magnitude of the interaction. (Note: for nonpolymeric macromolecules, molecular size essentially determines the correlation length ξ . However, for large flexible polymers in solution, the decay length is established by volume fraction and ‘quality’ of the solvent – refs [22] and [30].) Because of the exponential dependence on separation, the potential contributed by depletion forces scales as $\Pi_M \xi$. Hence, concentrated solutions of large polymers can produce strong aggregation of membrane capsules and cells. For example, adhesion of lipid bilayer vesicles in concentrated solutions of dextran and polyethylene oxide polymers demonstrates an enormous increase in potential for aggregation with smooth surfaces (fig. 7). Although much weaker than polymer-driven adhesion, the potential

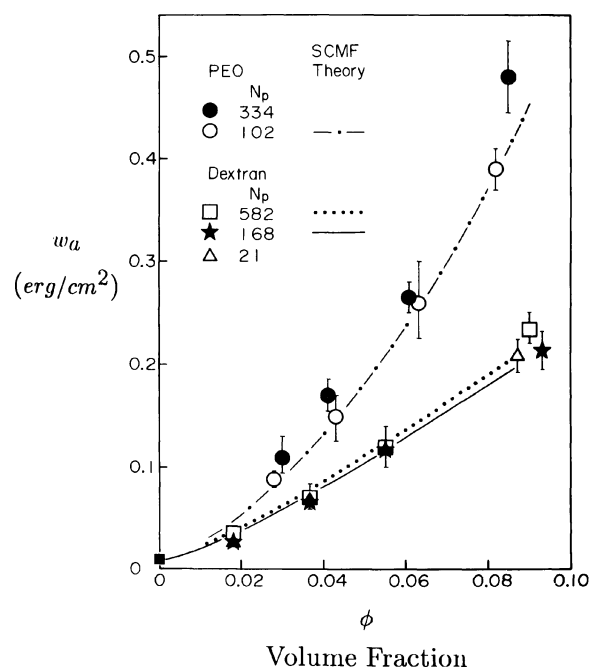


Fig. 7. Free energy potentials (adhesion energies) for adhesion of neutral lipid bilayer vesicles in concentrated solutions of nonadsorbing polymers (dextran and polyethylene oxide PEO). Curves are predictions for the 'depletion' interaction derived from Self Consistent Mean-Field SCMF theory [22]. The intercept at zero volume fraction is the level of adhesion energy produced by Van der Waals forces between the neutral vesicle surfaces. Note: there is no dependence on the size N_p (number of monomer segments) of the soluble polymer as expected for this 'semi-dilute' regime in good solvent conditions.

for lipid bilayer vesicle adhesion in plasma proteins (albumin and fibrinogen) also increases in direct proportion to osmotic pressure of the protein solution and protein dimension [22].

In contrast with smooth lipid bilayers, aggregation of red blood cells in concentrated polymer and fibrinogen solutions is characterized by much lower adhesion energies ($\sim 10^{-3}$ – 10^{-2} erg/cm²); no aggregation is seen in monomeric albumin solutions. Clearly, the important factor is interfacial structure. For cell surfaces, small molecules like albumin easily penetrate into the glycocalyx to greatly diminish depletion whereas larger species like fibrinogen are excluded from the glycocalyx to extend depletion. This explains why aggregation occurs when polymers of albumin are present. For cell surfaces, the potential for adhesion is reduced both by penetration of the solute into the glycocalyx and electrostatic repulsion between superficial charges. In relation to biology, the important feature is that environments of concentrated proteins in sera and connective tissue gels can contribute 'pressures' to draw surfaces closer together when protein solutes are excluded from contact zones. For example, agglutination of cells by antibodies is strongly enhanced in concentrated solutions of nonadsorbing polymers [31]. Similarly, ineffective agglutinins and viruses are often 'potentiated' by polymer solutions [32].

A universal feature of depletion forces is that they lead to ideal adhesion where adhesion energy matches separation (fracture) energy. For example, red cells are elastically deformed by contact spreading in polymer solutions (fig. 8); tension builds-up in the membrane to oppose the adhesion potential. Spontaneity of spreading and cell body deformation is an obvious 'signature' of ideal adhesion which – if observed – immediately points to the long range nature of attraction between the surfaces. Unfortunately, this behavior is seldom (almost never!) seen in biological

Fig. 8. Spontaneous adhesion and spreading of a red blood cell onto a sphered red cell surface in a concentrated solution of high molecular weight dextran polymer. Note: the 'ideal' character of the adhesion process is demonstrated by the elastic deformation of the cell where the membrane 'spreading' tension is on the order of the adhesion energy (10^{-3} – 10^{-2} erg/cm²).

cell adhesion.

5. Biological adhesion: Contact formation

For biological functions that involve interactions between cells, nature has chosen to suppress the labile-spontaneous action of colloid forces. Attraction is restricted to focal-molecular bonding with no apparent long range contribution from Van der Waals forces. As such, cells seem well stabilized against nonspecific adhesion. The universal presence of a thick (~ 100 Å) extrafacial ‘forest’ of sugar peptides establishes a significant steric barrier – enhanced by electrostatic repulsion local to the periphery. In addition to molecular roughness, cells usually exhibit large contour roughness in the form of wrinkles – folds – spikes. The contour or ‘topographical’ roughness is driven by tectonic contraction of the cytoskeletal structure in the cell cortex. The strong steric impedance to adhesion is augmented by mechanical rigidity of the cortex which enables cells to easily avoid adhesion except at very localized promontories. To form large contact areas, a smoothing process is required to achieve high densities of molecular attachments. Here, nature has developed cell motility as the mechanism to spread contact and to smooth-out interfacial asperities (examples shown in fig. 9). Even so, adhesive contacts between biological cells often appear irregular with many unbound (defect) regions and infrequent attachments between surfaces. Irregular contacts should compromise the strength of adhesion. However, cell-cell contacts are usually strong and difficult to separate. Since initial contact formation originates primarily from active cell motility *or* external mechanical impingement, the central question is what determines the strength of adhesion in biology?

5.1. Spreading by cytoskeletal contraction

More subtle than cell motility (amoeboid ‘crawling’), receptor-cytoskeletal ‘coupling’ in cells provides another mechanism to spread contact. The action requires that contractile stresses (tensions) in the subsurface cortical network be transmitted to the intersurface attachments through receptor linkages and that cortical contraction outside of the contact region be much stronger than inside the contact. This differential contraction in the cortex creates a *mechanical* spreading energy given by excess contractile tension $\Delta\tau_N$ in the network. As such, mechanical equilibrium is again approximated by a ‘Young–Dupre’ relation,

$$\Delta\tau_N = (\tau_{Bl} + \tau_N)(1 - \cos\theta_c) \quad (5)$$

where $\tau_m = \tau_{Bl} + \tau_N$ is the total tension contributed by bilayer and network forces, respectively. In this way, binding of cell surface receptors can signal a mechanical transduction to spread contact and stress the adherent cell. To a casual observer, the response would seem like ideal ‘wetting’ (as if driven by a true adhesion energy); but actually the process is driven by cytoskeletal action. An amplifying feature is that surface roughness is diminished to simultaneously promote recruitment of new

Fig. 9. Examples of the ‘universal’ mechanism that drives biological cell contact formation: video micrographs of a blood granulocyte actively (a) spreading on an endothelial cell surface and (b) engulfing a yeast pathogen.

adhesive attachments and strengthen adhesive contact. Differential contraction in membrane cytoskeletal structures may be an essential mechanism for separation of different cell types in tissue development. Such a mechanism could account for the ‘apparent’ surface energy driven organization of mixed-cell aggregates that was observed many years ago [36]. A major ‘clue’ is that the ‘apparent’ surface energies deduced from measurements of interfacial tension [36] were quite large $\sim 1 \text{ erg/cm}^2$, too large (by at least 10^2 !) to have been created by equilibrium attachments between cell surface receptors. On the other hand, differential contraction in the cytoskeletal structure of cells *can* easily produce mechanical energies of $\sim 1 \text{ erg/cm}^2$.

6. Biological adhesion: Focal bonding

Unlike long range colloid forces that are distributed uniformly over surfaces, *specific* bonding between cell surface receptors is localized to microscopic sites (either by soluble ligand bridges or direct receptor-receptor bonds). Most likely, the range of the direct bonding force is only ‘atomic’ in scale. However, conformational flexibility and thermal motion combine to extend the range of bonding force. Even so, the attachment remains focal in character where attraction is perhaps active only over distances of a few nanometers. Again different from colloid interactions, the

'physics' of specific molecular bonding cannot be expressed in terms of a universal potential of mean force. Conceptually, local atomic structure of the binding domain governs the direct interaction which is most easily represented by a short range contact potential. On the other hand, it is the conformational stiffness of the receptor and ligand that regulate the actual range of action. As such, unpredictable variations in strength and range easily arise in specific adhesive interactions. Thus, bonding is principally characterized by a thermodynamic affinity for bond formation at contact and a phenomenological rupture force that represents the strength of attachment. Conceptually, the rupture force should be the maximum gradient in the effective bonding potential. However, attachments may fail by several possible mechanisms: i.e. bond dissociation, internal 'fracture' of molecules, extraction of receptors from the membrane, etc. The question is what microscopic actions govern the strength of attachment?

6.1. Strength of attachment

A significant 'clue' to microscopic determinants of adhesive strength has come from measurements [13] of discrete forces required to rupture focal attachments between red blood cells as demonstrated in fig. 10.³ As shown in fig. 11, the rupture forces

Fig. 10. Video micrograph of a micromechanical measurement of rupture strength for a molecular-point attachment between red blood cell surfaces (formed by an agglutinin cross bridge). Displacement Δx of the pressurized cell on the left provides a direct measure of the force applied to the focal attachment site. Note: the force at detachment was order 10^{-6} dyn (10^{-11} N) and was determined from the membrane tension τ_m plus the displacement Δx (i.e. $f \sim \tau_m \Delta x$).

³ To isolate microscopic attachments, a pressurized-spherical red cell was 'touched' to a chemically-fixed test cell surface prebound with agglutinin. By significantly reducing the level of agglutinin bound to the test cell, touching at a point only resulted in adhesion in about half of the attempts. This statistic implied that focal adhesion involved only 1 or 2 microscopic agglutinin bridges. When the pressurized

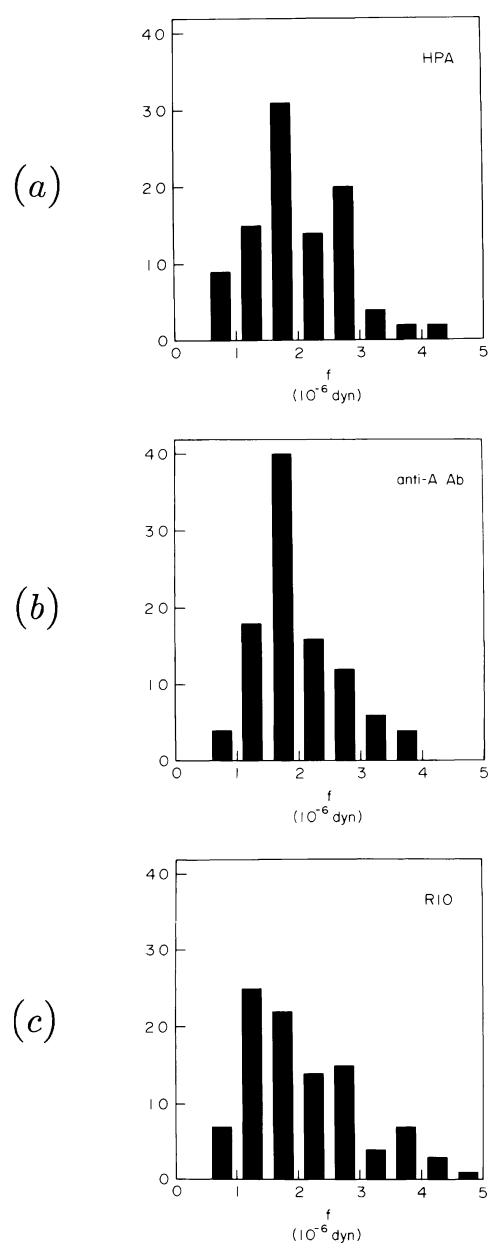


Fig. 11. Summary of forces measured for rapid detachment ($< 1-5$ sec) of red blood cells bonded at microscopic points by three different agglutinins. The cells were retracted at a steady rate of $0.4 \mu\text{m}/\text{sec}$. The histograms cumulate results from tests with cells attached by the following agglutinins: (a) the snail lectin HPA and (b) anti-A serum both of which bind to blood type A antigens (thought to be mostly glycolipids); (c) R10 monoclonal antibody to red cell glycoprotein A (a membrane integral protein).

cell was retracted by the pipet (fig. 10), the small attachment force deformed the cell until rupture

grouped around a common value of $1-2 \times 10^{-6}$ dyn (10^{-6} dyn = 10^{-11} N) for several agglutinins (lectin, monoclonal antibody, polyclonal sera) with no obvious dependence on bond chemistry. Surprisingly, this magnitude of rupture force ($\sim \mu$ dyn) is an order of magnitude below values expected for weak hydrogen bonds and well below stronger types of chemical forces! What type of failure process could be so weak and nonspecific in character? The evidence strongly indicated that single molecular attachments (receptors) were extracted from the lipid bilayer core of the membrane. To examine this hypothesis, a comparative fluorescence assay was devised in which either the agglutinin was prepared in advance with a fluorescent label *or* the proteins in a native cell membrane were chemically conjugated with a fluorescent label. Then with each type of label preparation, large contact areas were produced by mechanical impingement of the native red cell against a chemically-rigidified test cell studded with agglutinin. The contacts were separated and the fluorescent 'footprints' left by the labelled constituents were examined to determine the locus of 'fracture'. The results clearly demonstrated that the agglutinin remained bound to receptors and that receptors were extracted from the native cell membrane [13, 31]. In engineering language, fracture of the adherent contact was obviously cohesive material failure not adhesive failure! Interestingly, the appropriate magnitude for the force (to pull a receptor out of a lipid bilayer) was predicted many years ago from simple considerations [33]. Based on theoretical concepts, the force should scale with the perimeter of the attachment (the square root of the number of hydrophobic membrane spanning sequences that form the attachment site) which is relatively insensitive to receptor structure. The lipid bilayer anchoring force establishes a universal threshold for rupture of the focal attachments between cell membranes *unless* adhesive bonds are extremely weak. Most likely, the major determinant of attachment strength is the presence *or* absence of linkage to the cortical cytoskeleton underneath the membrane. Because of the low value of the lipid bilayer anchoring force, it is likely that transient encounters between cells of the immune system and other cells may involve transfer of microscopic components from the weakest cell interface to the strongest. This could be a direct mechanism for cellular communication and perhaps important in 'recognition'.

occurred. The observed displacement Δx at the time of rupture provided a direct measure of the peak force for the microscopic contact as readily determined from a simple mechanical proportionality,

$$f_n = k_{\text{RBC}} \Delta x.$$

The elastic 'spring constant' k_{RBC} for red cell extension is approximated by,

$$k_{\text{RBC}} \simeq 2\pi \cdot \tau_m / \{ \ln(2R_0/R_p) + \ln(R_0 \sqrt{\tau_m/k_c}) \},$$

$$\tau_m = \Delta P \cdot R_p / 2[1 - R_p/R_0],$$

where P is the pipet suction applied to pressurize the deformable cell; R_p , R_0 are radii of the pipet lumen and outer spherical portion of the cell, respectively.

6.2. Microscopic dynamics of rupture

Dynamics enters into the mechanics of contact fracture in two ways: First, forces that separate cell contacts act through the viscous materials of cell structure. Second, the microscopic failure of focal attachments involves time-dependent random processes. Cell materials often dominate the time response when adherent cells are separated. In many situations, cell compliance and dissipation compromise mechanical analysis of cell adhesion experiments and lead to unfounded conclusions. However, cell material response is peculiar to cell structure and method of mechanical loading. Thus, these particular features will not be addressed here in order to focus on the more general impact of microscopic processes on dynamic behavior.

When considering microscopic actions, we must keep in mind that biological membranes are ‘soft’ – almost liquid like interfaces – where thermal excitations play a major role in all events. Consequently, the forces observed to rupture focal contacts represent the macroscopic outcome of stochastic events (evident from the spread of forces in fig. 11). A random process for failure of focal attachments is expected to depend on the number of molecular connections within the attachment, magnitude and duration of the externally-applied force, etc. Even for three variables (number of molecular connections, magnitude of the applied force, and time), theoretical description of the random process may not be trivial. However, a simple abstraction provides a rich venue for demonstrating major features of failure. In the simple model, failure is represented by a frequency ν or rate of failure (number of events/time) which is an average over a large ensemble of times to reach failure for single attachments exposed to a specific level of force f [13]. Conceptually, the frequency should increase as the applied force increases; but the dependence on force may be very complicated. Phenomenologically, ‘weak’ versus ‘strong’ dependence on force can be approximated by a power law [13],

$$\nu \approx \nu_0(f/f_0)^a \quad (6)$$

which involves three parameters: intrinsic rate ν_0 and force f_0 for failure, and an exponent ‘a’. For a stationary random process, the probability density for failure (the fraction of molecular attachments that fail within a small increment of time) should decay exponentially with time, i.e.

$$p(t, f) \approx \nu \cdot e^{-\nu t} = \nu_0 \left(\frac{f}{f_0} \right)^a e^{-\nu_0(f/f_0)^a t} \quad (7)$$

following an instantaneous application of force. However, the force can never be applied instantly so this is not the appropriate statistical density to predict experimental observations. In experiments, the force always builds-up at a finite rate, $f = \dot{f} \cdot t$, which implies that the probability density for failure of single molecular attachments will be peaked, i.e.

$$p(t, \dot{f}) \approx \nu_0 b (\nu_0 t)^a e^{-b(\nu_0 t)^{a+1}/a+1}, \quad (8)$$

$$b \equiv a(\dot{f}/\nu_0 f_0)^a.$$

The likelihood of failure increases initially with time and then decays exponentially. For constant rate of force increase, the forces at rupture in experiments should group around a 'most frequent' force \hat{f} that is derived from the time t' where the probability density is maximal (i.e. $\hat{f} = \dot{f} \cdot t'$),

$$\hat{f} \approx f_0(\dot{f}/a\nu_0 f_0)^{1/a+1}. \quad (9)$$

The 'most frequent' force is scaled by the intrinsic microscopic force f_0 that underlies the failure process; but the dynamics shows up in the statistics of failure. If the force gradient is steep near failure ($a \gg 1$), the rupture force will depend weakly on the rate of loading \dot{f} . As will be discussed, predictions of the simple microscopic rupture process are qualitatively consistent with the macroscopic dynamics of separation for large agglutinin-bonded regions between red blood cells.

7. Biological adhesion: Macroscopic contacts

As already noted, formation of large contact regions in biological adhesion is driven mainly by external processes (either cell motility or mechanical impingement). The localized action of bonding is obscured by the macroscopic dynamics of cell deformation as contact spreads. The principal resultant of bonding affinity is to establish the surface density \tilde{n}_B (number/area) of binding sites for intersurface attachments. However, the actual density \tilde{n}_a of attachments depends on several mesoscopic factors:

- (i) contour roughness and local mechanical stiffness of the membrane cortex;
- (ii) receptor diffusion and convective transport;
- (iii) receptor-cytoskeletal linkage and cytochemical 'induction' (e.g., active insertion and deletion of membrane receptors);
- (iv) steric hindrance by large surface moieties; etc!

Any of these factors can significantly alter the density of attachments. However, one physical factor will be emphasized because it clearly regulates the patency and strength of all cell adhesive contacts: mesoscale roughness and mechanical stiffness.

7.1. Contour roughness, mechanical stiffness and impingement

Topographical roughness is a prominent characteristic of all cell surfaces (even the seemingly-smooth red blood cell) since wrinkles and other irregularities are produced in the plasma bilayer as a consequence of cortical contraction and structure. These mesoscale contour variations lead to geometric frustration of intersurface attachments. The frustration is compounded by local mechanical rigidity which can prevent the surface from being smoothed by adhesion at promontories. Ideally, the surface pressure of bound receptors should promote contact spreading. For typical values of receptor density on the order of $< 10^{11}/\text{cm}^2$, the maximum spreading pressure is of order $< 4 \times 10^{-3} \text{ erg}/\text{cm}^2$. The spreading action must exceed the local mechanical opposition to deformation in order to smooth the surface. Even in the absence of stiffness from the cytoskeletal cortex, the mechanical energy threshold will

be at least the order of membrane bending energy, i.e. k_c/R_c^2 , where $1/R_c$ is the characteristic curvature for a small promontory ($> 10^5 \text{ cm}^{-1}$). Given that $k_c > 10^{-12} \text{ erg}$, the bending energy $k_c/R_c^2 \sim 10^{-2} \text{ erg/cm}^2$ will exceed the equilibrium potential for contact spreading. (Similarly, fluctuations in local curvature driven by thermal bending excitations can only advance contact when $\tilde{n}_B kT > k_c/R_c^2$.) Hence, roughness becomes trapped by mechanical stiffness – not restricted by lateral mobility of receptors – and is frozen by bonding at the promontories.

Mesoscale roughness and mechanical stiffness clearly impede contact formation and moderate strength of adhesion when red cells are agglutinated by multivalent (bridging) antibodies and lectins [31]. These features are demonstrated in the video microscope images shown in fig. 12. Here, driven by mechanical impingement, large contact regions were agglutinated between red blood cells by monoclonal antibodies

Fig. 12. Video micrographs of micromechanical assembly and detachment of a normal red blood cell to/from a chemically-rigidified red cell prebound with agglutinin molecules (monoclonal antibodies or lectins). The cells were maneuvered to touch and adhered focally but did not spread spontaneously. Subsequent to mechanical impingement (a), the flaccid red cell was detached (b) from the rigid cell by pipet suction. Note the tenacious attachment as evidenced by extreme deformation of the flaccid cell.

and then separated.⁴ As the cells were separated, the peeling tension had to be increased progressively to reduce the contact dimension as shown in fig. 13. Because the detachment angle θ_c remained close to 90° , the peeling tension at the perimeter provided a direct measure of the fracture energy w_f . Consistent with the absence of spontaneous spreading, the initial level of tension was very low ($< 10^{-2}$ dyn/cm); but tensions of ~ 1 dyn/cm were necessary to fully detach the cell. The first surprise was that over the thirty-fold range of separation rates accessible to experiment (detachment from seconds to minutes), there was no detectable change in fracture energy! The other surprise was the absence of specific dependence on the type of agglutinin! Progressive strengthening of adhesion with separation appeared to be nonspecific (governed only by the amount of agglutinin prebound to the test cell and magnitude of impingement pressure) and insensitive to peeling rate. There was a clear phenomenological message: an important physical mechanism amplifies adhesive strength as biological cell contacts are separated!

Discussed earlier, the microscopic origin of strength for these agglutinin attachments appeared to be lipid bilayer ‘anchoring’ with a common magnitude for rupture force. Taking the rupture force for a single attachment site as constant and of order $\sim 1\text{--}2$ μ dyn, it was deduced that the maximum level of peeling tension (~ 1 dyn/cm) corresponded to complete bonding of all agglutinin sites local to the contact perimeter. This follows from the maximum number of agglutinin receptors per length of contact given by the square root of surface density; the surface density $\tilde{n}_B \sim 10^6/\text{red}$ blood cell implies the maximum number per length of $10^2/\mu\text{m}$. By comparison, the number of attachments per length of perimeter consistent with the low values of tension at the beginning of contact separation (~ 0.01 dyn/cm) would be only a few attachments (< 10) per μm ! The comparison shows that amplification of fracture strength arises from major recruitment of microscopic attachments. What immediately comes to mind is accumulation of receptors driven by lateral forces tangent to the membrane (i.e. drag of receptors into the contact zone). Indeed, this often happens when adherent cells are separated [35]. However, for the tests illustrated in fig. 12 (and the results in fig. 13), proteins in the substrate cell had been chemically cross-linked [31]. Thus, the amplification of adhesive strength resulted from a different mechanism. Most likely, attachments were recruited by smoothing interfacial roughness interior to the contact as the cells were separated. Compelling evidence for this hypothesis is the frequent macroscopic observation that large-trapped fluid pockets (‘blisters’) disappear from a contact zone during separation. Similarly, numerous mesoscopic defects (irregular attachment) have been seen along adhesive

⁴ In these tests, a chemically rigidified red blood cell (preswollen to form a sphere) was used as an adhesive substrate for attachment of a normal red blood cell. To maximize the availability of attachment sites, monoclonal antibodies or lectins were bound at saturation only to the test particle surface in advance of the experiment. The normal red cell was not exposed to the agglutinin until surface contact. The normal red cell was maneuvered by micropipet to touch the agglutinin studded cell, but the cell only adhered to the test cell at a focal site without spreading. To produce large regions of contact, mechanical impingement was required as shown in fig. 12a. Finally, the flaccid cell was separated from the test cell by mechanical suction into the pipet (fig. 12b). The peeling tension at the perimeter of contact was derived from the suction pressure by straightforward mechanical analysis [34].

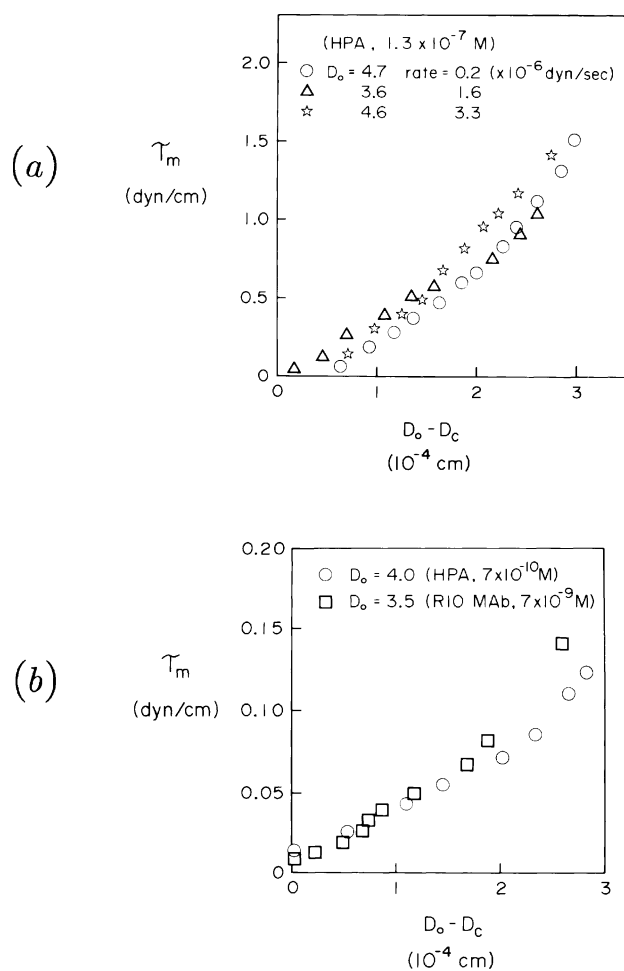


Fig. 13. Fracture energies (given by peeling tension τ_m) plotted versus separation (reduction in contact dimension) for red cell pairs agglutinated by monoclonal antibodies (R10) and snail lectin (HPA) which bind to different membrane receptors. The agglutinin concentrations used to precoat each test cell are given for both sets of experiments. (a) The fracture process appears to be insensitive to the rate of cell detachment. (b) The fracture process appears to be 'nonspecific' with no recognizable dependence on the chemically different agglutinins.

contacts in electron micrographic sections of agglutinated cells [37]. Consistently, mechanical analysis (to be described next) shows that a local mechanical pressure exists to push the surfaces together inside the contact region. Furthermore, the local compression of the contact is accompanied by lateral shear of the membrane relative to the substrate. Clearly, local impingement and tangential smoothing of interfacial roughness will lead to new attachments. The important lesson is that mechanical impingement and interfacial smoothing are *inherent* to the mechanical process of separation for flexible membranes.

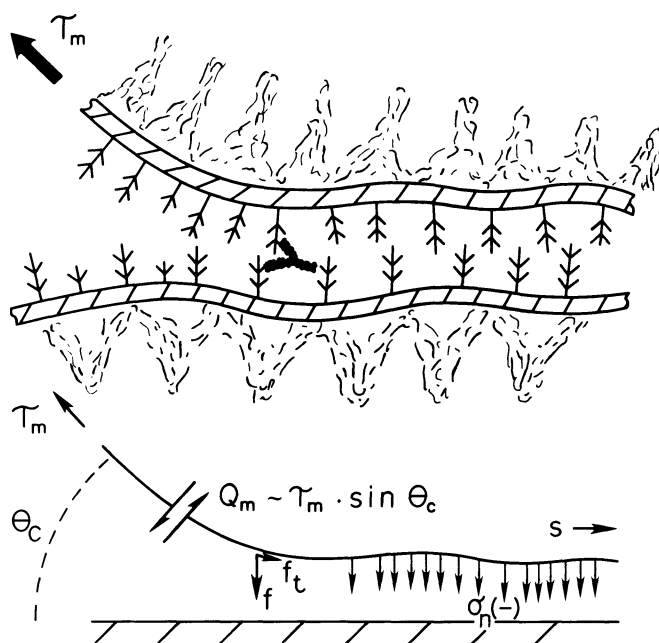


Fig. 14. Schematic of ‘mesoscale’ fracture for membranes bonded by focal-molecular attachments (symbolized by ‘Y’ in the upper sketch). Membrane bending stress Q_m at the perimeter of the contact creates the force f to detach the focal bond and a tangential force f_t acts to drag the attachments into the contact. Bending about the focal bond leads to a normal-compressive stress σ_n (pressure) that pushes the surfaces together.

7.2. Mesoscale mechanics of fracture

The mechanics of fracture couples macroscopic peeling tension to microscopic attachment forces. The macroscopic consequence of focal bonding is that mechanical stresses (tension and stresses normal to the surface) appear to be discontinuous at the perimeter of the contact region [10]. However, in a conceptually magnified view (as illustrated in fig. 14), membrane tension remains continuous along the contour; the detachment force f is produced by local bending stress derived from gradients (dc_m/ds) of membrane curvature, i.e.

$$Q_m \approx k_c \frac{\partial c_m}{\partial s} \approx f \sqrt{\tilde{n}_a}. \quad (10)$$

The attachment force per length of perimeter is $\sqrt{\tilde{n}_a} \cdot f$ given the surface attachment density \tilde{n}_a . In turn, local bending stresses are coupled to the macroscopic peeling tension τ_m through a leverage factor $\sin \theta_c$; again θ_c is the ‘apparent’ contact angle observed macroscopically. As such, the peeling tension becomes proportional to the average bond force along the perimeter, i.e.

$$\tau_m \sin \theta_c \approx f \sqrt{\tilde{n}_a}. \quad (11)$$

Two mechanical corollaries accompany the relation between tension and attachment force. First of all, the peeling tension creates small lateral forces f_t on attachments (as well as direct extensional forces f). The lateral force is produced by a small deviation of the detachment force from the local membrane normal (i.e. the surfaces are not exactly parallel at the perimeter of the contact). From mechanical analysis [10], the deviation angle θ^* and the lateral force $f_t \sim f \cdot \theta^*$ are predicted to depend on membrane bending stiffness and the effective range l_B for action of single attachments. The result is that the deviation angle is a very weak function of peeling tension,

$$\theta^* \sim l_B^{1/2} (\tau_m / k_c)^{1/4}.$$

Hence, the lateral force is essentially proportional to peeling tension but small in magnitude. In the absence of cytoskeletal restrictions, these lateral forces drive receptors to accumulate at the contact perimeter.

Second, peeling produces a normal-compressive pressure on the membrane interior to the contact. Attachments along the perimeter form a ‘fulcrum’ around which membrane bending forces create an impingement pressure inside the contact. This pressure pushes the membrane surface towards the substrate surface over a narrow region d_c (governed by the bond extension l_B and local radius of curvature – R_c) with a magnitude σ_n that scales as,

$$d_c \sim l_B^{1/2} (k_c / \tau_m)^{1/4},$$

$$\sigma_n \sim -Q_m / d_c \sim -\tau_m (\tau_m / k_c l_B^2)^{1/4}.$$

The impingement pressure easily reaches the level of 1 Atm (10^6 dyn/cm²) when tensions are large (~ 1 dyn/cm). Importantly, impingement locally smoothes the irregular membrane contour and promotes recruitment of new attachments inside the contact zone.

The mesoscale mechanics predicts that peeling tensions should lie between specific bounds: i.e. a minimum level of tension below which the membrane contact can spread by local bonding *and* a maximum level of tension above which the membrane is detached from the substrate. The ‘adiabatic’ (kinetically-trapped) mechanical limits expose the *nonideal* character of the adhesion process and are expressed by the following inequality (neglecting trigonometric factors of contact angle):

$$k_c l_B^2 \tilde{n}_B^2 < \tau_m < \hat{f} \sqrt{\tilde{n}_a}.$$

Therefore, the membrane tension ranges between a lower value governed by the paucity of attachments and an upper value established by the peak force \hat{f} required to rupture attachments. The lower bound is dictated simply by the requirement that the curvature of the membrane contour proximal to the contact perimeter must be ‘flattened’ sufficiently to allow formation of new attachments at a distance of $(1/\tilde{n}_a)^{1/2}$ beyond the perimeter *and* within the range l_B of bonding action. When

practical values are introduced for these parameters, the level of tension compatible with contact spreading is less than 10^{-3} dyn/cm. By comparison, the level of tension necessary to peel the contact apart can easily reach 1 dyn/cm when microscopic rupture forces are on the order of 10^{-6} dyn or more. Phenomenologically, the *strength* of adhesion is determined by both the rupture force \hat{f} and the density \tilde{n}_a of attachment sites. If the attachment strength remains constant throughout contact separation, the level of tension required to separate an adhesive contact will be governed primarily by the local density of attachments. As already emphasized, the subtle aspect is that the rupture force \hat{f} may be unrelated to the chemistry of the bond that initiated attachment. The rupture force measures the failure of the weakest component in the adhesion complex!

8. Summary comment

As described in the text, biological cell adhesion is a complex situation which (except in rare cases) cannot be treated as an ideal 'wetting-like' process. Consequently, it is not possible to write down a set of universal 'laws' that explicitly cover all cell adhesion phenomena. The objective here has been to expose unconventional features of biological cell adhesion and to relate microscopic actions to macroscopic behavior. Although important aspects have been overlooked, major physical determinants have been identified which are expected to be involved in every cell adhesion process.

Acknowledgement

The author gratefully acknowledges the support of the US National Institutes of Health through grants HL45099, HL31579, and the Canadian Medical Research Council through grant MT7477. The author is an Associate in the 'Science of Soft Surface and Interfaces' Program sponsored by the Canadian Institute for Advanced Research.

References

1. Springer, T.A., 1990, *Nature* **346**, 425.
2. Ruoslahti, E. and M.D. Pierschbacher, 1987, *Science* **238**, 491.
3. Kishimoto, T.K., R.S. Larson, A.L. Gorbi, M.L. Dustin, D.E. Staunton and T.A. Springer, 1990, in: *Leukocyte Adhesion Molecules*, eds T.A. Springer et al. (Springer, New York) p. 7.
4. Lawrence, M.D. and T.A. Springer, 1991, *Cell* **65**, 859.
5. Cunningham, B.A., J.J. Hemperly, B. Murray, E.A. Prediger, A. Brackenbury and G.M. Edelman, 1987, *Science* **236**, 799.
6. Dustin, M.L. and T.A. Springer, 1991, *Annu. Rev. Immunol.* **9**, 27.
7. Takeichi, M., 1991, *Science* **251**, 1451.
8. Magee, A.I. and R.S. Buxton, 1991, *Curr. Opin. Cell Biol.* **3**, 854.
9. Adamson, A.W., 1982, *Physical Chemistry of Surfaces* (Wiley, New York).
9. Bell, G.I., M. Dembo and P. Bongrand, 1984, *Biophys. J.* **45**, 1051.
9. Hammer, D.A. and D.A. Lauffenburger, 1987, *Biophys. J.* **52**, 475.
9. Cozens-Roberts, C., D.A. Lauffenburger and J.A. Quinn, 1990, *Biophys. J.* **58**, 841.
10. Evans, E.A., 1985, *Biophys. J.* **48**, 175.
10. Dembo, M., D.C. Torney, K. Saxman and D.A. Hammer, 1988, *Proc. R. Soc. London Ser. B* **234**, 55.

11. Jacobson, K., A. Ishihara and R. Inman, 1987, *Annu. Rev. Physiol.* **49**, 163.
Vaz, W.L., Z.I. Derzko and K.A. Jacobson, 1982, *Cell Surf. Rev.* **8**, 83.
12. Capo, C., F. Garrouste, A.-M. Benoliel, P. Bongrand, A. Ryter and G.I. Bell, 1982, *J. Cell Sci.* **56**, 21.
13. Evans, E.A., A. Leung and D. Berk, 1991, *Biophys. J.* **59**, 838.
14. Evans, E. and R. Skalak, 1980, *Mechanics and Thermodynamics of Biomembranes* (CRC Press, Boca Raton, FL).
Flügge, W., 1966, *Stresses in Shells* (Springer, New York).
15. Evans, E., 1990, **43**, 327.
16. Bloom, M., E. Evans and O.G. Mouritsen, 1991, **24**, 293.
17. Evans, E.A., 1980, *Biophys. J.* **30**, 265.
Skalak, R., P.R. Zarda, K.-M. Jan and S. Chien, 1981, *Biophys. J.* **35**, 771.
18. Seifert, U. and R. Lipowsky, 1990, *Phys. Rev. A* **42**, 4768.
19. Verwey, E.J.W. and J.Th.G. Overbeek, 1948, *Theory of the Stability of Lyophobic Colloids* (Elsevier, Amsterdam).
20. Parsegian, V.A., 1975, in: *Physical Chemistry: Enriching Topics from Colloid and Surface Chemistry*, eds J. van Olphen and K.J. Mysels (Theorex, La Jolla, CA) p. 27.
Mahanty, J. and B.W. Ninham, 1976, *Dispersion Forces* (Academic Press, London).
21. Israelachvili, J., 1985, *Intermolecular and Surface Forces* (Academic Press, San Diego, CA).
22. Evans, E. and D. Needham, 1988, *Macromolecules* **21**, 1822.
Evans, E., 1989, *Macromolecules* **22**, 2277.
Evans, E., D. Needham and J. Janzen, 1987, in: *Proteins at Interfaces*, eds J.L. Brash and T.A. Horbet, ACS Symposium Series **343**, 88.
23. Evans, E. and D. Needham, 1987, *J. Phys. Chem.* **91**, 4219.
24. LeNeveu, D.M., R.P. Rand, V.A. Parsegian and D. Gingell, 1977, *Biophys. J.* **18**, 209.
Parsegian, V.A., N.L. Fuller and R.P. Rand, 1979, *Proc. Nat. Acad. Sci. USA* **76**, 2750.
25. Helfrich, W., 1978, *Z. Naturforsch.* **33A**, 305.
26. Lipowsky, R. and S. Leibler, 1986, *Phys. Rev. Lett.* **56**, 2541.
27. Evans, E. and V.A. Parsegian, 1986, *Proc. Nat. Acad. Sci. USA* **83**, 7132.
28. Evans, E., 1991, *Langmuir* **7**, 1900.
29. Lipowsky, R. and U. Seifert, 1991, *Langmuir* **7**, 1867.
30. Joanny, J.F., L. Leibler and P.G. de Gennes, 1979, *J. Polym. Sci. Polym. Phys. Ed.* **17**, 1073.
31. Evans, E., D. Berk, A. Leung and N. Mohandas, 1991, *Biophys. J.* **59**, 849.
32. Jandl, J.H. and W.B. Castle, 1956, *J. Lab. Clin. Med.* **47**, 669.
Haywood, A.M. and B.P. Boyer, 1986, *Biochemistry* **25**, 3925.
33. Bell, G.I., 1978, *Science* **200**, 618.
34. Berk, D. and E. Evans, 1991, *Biophys. J.* **59**, 861.
35. Evans, E. and A. Leung, 1984, *J. Cell Biol.* **98**, 1201.
Tozeren, A., K.-P. Sung and S. Chien, 1989, *Biophys. J.* **55**, 479.
36. Steinberg, M.S., 1970, *J. Exp. Zool.* **173**, 395.
Steinberg, M.S. and D.R. Garrod, 1975, *J. Cell Sci.* **18**, 385.
37. Coakley, W.T., L.A. Hewison and D. Tilley, 1985, *Eur. Biophys. J.* **13**, 123.